Boundary-Layer Meteorol (2007) 125:329–341
DOI 10.1007/s10546-007-9192-7

ORIGINAL PAPER

On the turbulent Prandtl number in the stable atmospheric boundary layer

Andrey A. Grachev · Edgar L Andreas · Christopher W. Fairall · Peter S. Guest · P. Ola G. Persson

Received: 6 September 2006 / Accepted: 24 March 2007 / Published online: 26 June 2007

Abstract This study focuses on the behaviour of the turbulent Prandtl number, Pr_t, in the stable atmospheric boundary layer (SBL) based on measurements made during the Surface Heat Budget of the Arctic Ocean experiment (SHEBA). It is found that Pr_t increases with increasing stability if Pr_t is plotted vs. gradient Richardson number, Ri; but at the same time, Pr_t decreases with increasing stability if Pr_t is plotted vs. flux Richardson number, Rf, or vs. $\zeta = z/L$. This paradoxical behaviour of the turbulent Prandtl number in the SBL derives from the fact that plots of Pr_t vs. Ri (as well as vs. Rf and ζ) for individual 1-h observations and conventional bin-averaged values of the individual quantities have built-in correlation (or self-correlation) because of the shared variables. For independent estimates of how Pr_t behaves in very stable stratification, Pr_t is plotted against the bulk Richardson number; such plots have no built-in correlation. These plots based on the SHEBA data show that, on the average, Pr_t decreases with increasing stability and $\mathrm{Pr}_t < 1$ in the very stable case. For specific heights and stabilities, though, the turbulent Prandtl number has more complicated behaviour in the SBL.

A. A. Grachev · P. O. G. Persson
Cooperative Institute for Research in Environmental Sciences,
University of Colorado,
Boulder, CO, USA

A. A. Grachev (✉) · C. W. Fairall · P. O. G. Persson
NOAA Earth System Research Laboratory,
Boulder, CO, USA
e-mail: Andrey.Grachev@noaa.gov

E. L Andreas
NorthWest Research Associates, Inc. (Bellevue Division),
Lebanon, NH, USA

P. S. Guest
Naval Postgraduate School,
Monterey, CA, USA

Keywords Richardson number · SHEBA · Stable boundary layer · Turbulent Prandtl number

1 Introduction

One major uncertainty in the atmospheric stable boundary layer (SBL) is associated with the stability dependence of the turbulent Prandtl number defined by

$$\mathrm{Pr}_t = \frac{k_m}{k_h} = \frac{\langle u'w' \rangle \frac{\mathrm{d}\theta}{\mathrm{d}z}}{\langle w'T' \rangle \frac{\mathrm{d}U}{\mathrm{d}z}} \equiv \frac{\varphi_h}{\varphi_m}, \tag{1}$$

where $k_m = -\frac{\langle u'w' \rangle}{\mathrm{d}U/\mathrm{d}z}$ is the turbulent viscosity, and $k_h = -\frac{\langle w'T' \rangle}{\mathrm{d}\theta/\mathrm{d}z}$ is the turbulent thermal diffusivity ($-\langle u'w' \rangle$ is the downwind stress component and $\langle w'T' \rangle$ is the temperature flux). The turbulent Prandtl number (1) describes the difference in turbulent transfer between momentum and sensible heat. Turbulent momentum transfer is more efficient than turbulent heat transfer when $\mathrm{Pr}_t > 1$ and vice versa. If the turbulent Prandtl number is not unity, Eq. 1 also demonstrates a difference between the stability profile functions of momentum, φ_m, and sensible heat, φ_h. These functions are defined as non-dimensional vertical gradients of mean wind speed, U, and potential temperature, θ:

$$\varphi_m = \frac{\kappa z}{u_*} \frac{\mathrm{d}U}{\mathrm{d}z}, \tag{2a}$$

$$\varphi_h = \frac{\kappa z}{T_*} \frac{\mathrm{d}\theta}{\mathrm{d}z}, \tag{2b}$$

where $u_* = \sqrt{-\langle u'w' \rangle}$ is the friction velocity, $T_* = -\langle w'T' \rangle / u_*$ is the temperature scale, and κ is the von Kármán constant. The turbulent Prandtl number is an important characteristic of momentum and heat turbulent mixing for calibrating turbulence models and other applications (e.g., Sukoriansky et al. 2006).

In spite of progress in understanding SBL physics, a unified picture on the stability dependence of Pr_t does not exist. First, we survey the experimental results. Kondo et al. (1978), Ueda et al. (1981), Kim and Mahrt (1992), Ohya (2001), Strang and Fernando (2001), and Monti et al. (2002) found that the turbulent Prandtl number increases with increasing stability on plotting Pr_t (or $1/\mathrm{Pr}_t$) vs. the gradient Richardson number, Ri. In plots of Pr_t vs. the stability parameter $\zeta = z/L$ (L is the Obukhov length and z is the measurement height), on the other hand, Howell and Sun (1999) found that Pr_t estimates are generally scattered around unity and do not strongly depend on stability. However, for the very stable regime ($\zeta > 1$), their estimates of the turbulent Prandtl number tended to be less than unity (their Fig. 9). Yagüe et al. (2001) reported a mixed result. According to their Fig. 10a, Pr_t increases (or $1/\mathrm{Pr}_t$ decreases) with increasing Ri; but they found no clear dependence of Pr_t on ζ (their Fig. 10b). Grachev et al. (2003, 2007) found Pr_t to decrease with increasing ζ. This finding is directly related to the different behaviours of φ_m and φ_h, Eqs. 2a and 2b, in the limit of very strong stability. According to Grachev et al. (2005, 2007), φ_m increases with increasing stability, whereas φ_h initially increases with increasing ζ, reaches a maximum at $\zeta \approx 10$, and then tends to level off with further increasing ζ.

Theoretical studies by Zilitinkevich and Calanca (2000), Zilitinkevich (2002), and Sukoriansky et al. (2006) and Beljaars and Holtslag's (1991) parameterization argue in favour of an increasing turbulent Prandtl number with increasing stability. Likewise, when Andreas (2002) reviewed seven different formulations for $\varphi_m - \varphi_h$ pairs in stable stratification, he found five predicted $\mathrm{Pr}_t = 1$ in very stable stratification and two predicted that Pr_t increased with increasing ζ. None predicted that Pr_t decreased. The result $\mathrm{Pr}_t > 1$ is usually associated with the presence of the internal gravity waves in the SBL. They are presumed to enhance the momentum transfer through pressure terms in the Navier–Stokes equations, whereas gravity waves do not affect the sensible heat flux (e.g., Monin and Yaglom 1971). However, the result $\mathrm{Pr}_t < 1$ was obtained in recent large-eddy simulation (LES) studies of the SBL. Beare et al. (2006) plotted the turbulent viscosity and the turbulent thermal diffusivity as a function of z. According to their Fig. 14, k_m is clearly less than k_h, corresponding to $\mathrm{Pr}_t < 1$ (note different scales on the horizontal axes for k_m and k_h in their Fig. 14). Also Basu and Porté-Agel (2006) reported $\mathrm{Pr}_t < 1$ from their LES simulations (p. 2082).

The purpose of this study is to examine how the turbulent Prandtl number depends on different stability parameters to shed light on the behaviour of Pr_t in the SBL.

2 Turbulent Prandtl number vs. different stability parameters

One may notice that authors who found the turbulent Prandtl number to increase with stability, i.e., $\mathrm{Pr}_t > 1$, (Kondo et al. 1978; Ueda et al. 1981; Kim and Mahrt 1992; Ohya 2001; Strang and Fernando 2001; Yagüe et al. 2001; Monti et al. 2002) plotted Pr_t (or $1/\mathrm{Pr}_t$) solely vs. the gradient Richardson number, defined by

$$\mathrm{Ri} = \frac{g}{\theta_v} \frac{\mathrm{d}\theta_v/\mathrm{d}z}{(\mathrm{d}U/\mathrm{d}z)^2} = \frac{\zeta \varphi_h}{\varphi_m^2}, \tag{3}$$

where θ_v is the virtual potential temperature of air and g is the acceleration due to gravity. On the other hand, those who reported $\mathrm{Pr}_t < 1$ (Howell and Sun 1999; Grachev et al. 2003, 2007) plotted Pr_t against the Monin-Obukhov stability parameter ζ defined by

$$\zeta = \frac{z}{L} = -\frac{z\, \kappa g \langle w' T_v' \rangle}{u_*^3\, \theta_v}. \tag{4}$$

In this context, the result obtained by Yagüe et al. (2001) is remarkable. As mentioned above, they found that Pr_t increased with increasing stability if Eq. 1 was plotted against Eq. 3; but the same data showed no clear stability dependence in Pr_t when Eq. 1 was plotted against Eq. 4. In the light of this result, it makes sense to use the same dataset to explore in detail how Pr_t depends on different indicators of stability.

Another widely used stability parameter, along with Eqs. 3 and 4, is the flux Richardson number defined by

$$\mathrm{Rf} = \frac{g}{\theta_v} \frac{\langle w' T_v' \rangle}{\langle u' w' \rangle (\mathrm{d}U/\mathrm{d}z)} \equiv \frac{\zeta}{\varphi_m}. \tag{5}$$

Near the surface, when surface temperature is available, it is convenient also to use a bulk Richardson number:

$$\mathrm{Ri}_B = -\frac{gz}{\theta_v}\frac{(\Delta\theta + 0.61\theta_v \Delta q)}{U^2}, \tag{6}$$

where $\Delta\theta$ and Δq are differences in the potential temperature and the specific humidity, respectively, between the *surface* and reference level z.

In this study, measurements of atmospheric turbulence made during the Surface Heat Budget of the Arctic Ocean experiment (SHEBA) are used to examine the turbulent Prandtl number, Eq. 1, as a function of four different stability parameters, given by Eqs. 3–6. Turbulent fluxes and mean meteorological data were continuously measured at five levels, nominally 2.2, 3.2, 5.1, 8.9 and 18.2 m (or 14 m during most of the winter), on the 20-m main SHEBA tower. This stood on sea ice in the Beaufort Gyre from October 1997 through September 1998 and yielded 11 months of data.

Each level on the main tower had a Väisälä HMP-235 temperature and relative humidity probe and an Applied Technologies, Inc. (ATI) three-axis sonic anemometer/thermometer, which sampled at 10 Hz. The surface temperature (necessary for computing Ri_B) was obtained from down-looking and up-looking Eppley broadband, hemispherical radiometers (model PIR). Turbulent covariance values and appropriate variances at each level are based on 1-h averaging and derived through frequency integration of the cospectra and spectra. Observations with a temperature difference between the air and the snow surface less than 0.5°C and wind speed smaller than $1\mathrm{ms}^{-1}$ have been excluded from our analysis to avoid the large uncertainty in determining the turbulent fluxes. Other relevant information on flux and profile measurements and calculations including quality-control criteria, can be found in Persson et al. (2002), Grachev et al. (2005, 2007), and Andreas et al. (2006).

Figure 1 shows the turbulent Prandtl number as a function of the stability parameters (3)–(5) for the same SHEBA dataset. The averaged points in Fig. 1 based on the conventional bin-averaging of the individual 1-h data for Pr_t and proper stability parameters are indicated by different symbols for each measurement level. The individual 1-h-averaged data based on the median fluxes and other medians (heights, temperatures, etc.) for the five levels are also shown in Fig. 1 as background x-symbols. These points give an estimate of the available data at all levels and the typical scatter of the data. In the case when data at all five levels are available, the medians represent the level 3 data.

The results presented in Fig. 1, though, are contradictory. The turbulent Prandtl number increases with increasing stability if Pr_t is plotted vs. Ri (Fig. 1a); but at the same time, Pr_t decreases with increasing stability if Pr_t is plotted vs. Rf (Fig. 1b) or vs. ζ (Fig. 1c).

Vertical gradients of the mean wind speed, potential temperature and specific humidity appeared in Pr_t, Ri, and Rf (Eqs. 1, 3, and 5) in Fig. 1 and were obtained by fitting a second-order polynomial through the 1-h profiles followed by evaluating the derivative with respect to z for levels 1–5 (Grachev et al. 2005, their Eq. 8). In Fig. 2, the vertical gradients at levels $n = 2$–4 that appear in Pr_t, Ri, and Rf are based on linear interpolations of mean wind speed and potential temperature derived from the two adjoining levels $n - 1$ and $n + 1$. Figure 2 confirms the results in Fig. 1 and, therefore, shows that the results in Fig. 1 are not sensitive to how we evaluated the wind speed and temperature gradients.

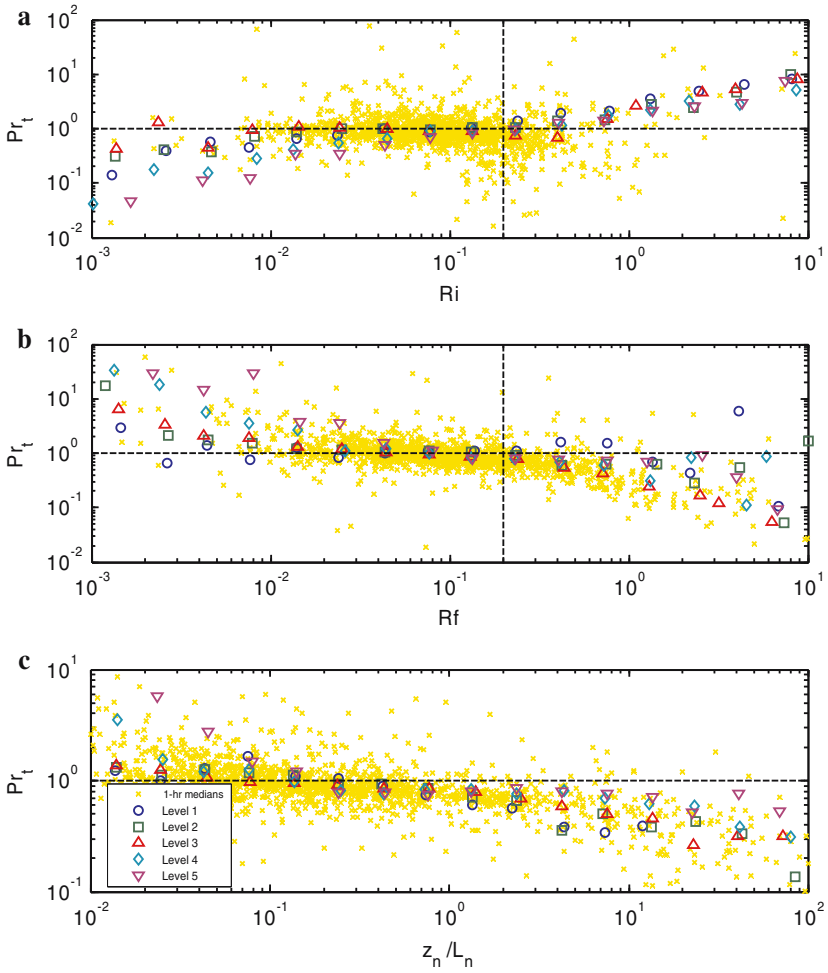

Fig. 1 Plots of the bin-averaged turbulent Prandtl number (bin medians) as functions of (**a**) Ri, (**b**) Rf, and (**c**) z_n/L_n (bin means) during the 11 months of the SHEBA measurements. The vertical dashed lines correspond to the critical Richardson number 0.2. Individual 1-h averaged data based on the median fluxes for the five levels are shown as background crosses

Thus we have a contradictory picture. On the one hand, according to Figs. 1a and 2a, the SHEBA data suggest that $\mathrm{Pr}_t > 1$ in the SBL, and this result agrees with findings reported by Kondo et al. (1978), Ueda et al. (1981), Kim and Mahrt (1992), Ohya (2001), Strang and Fernando (2001), and Monti et al. (2002). On the other hand, the SHEBA data also support the opposite opinion, $\mathrm{Pr}_t < 1$ (Figs. 1b, c, 2b, c).

3 Self-correlation

The above contradiction is likely associated with self-correlation. The problem is that the two quantities–for example, φ_m and ζ or Pr_t and Ri—between which a functional

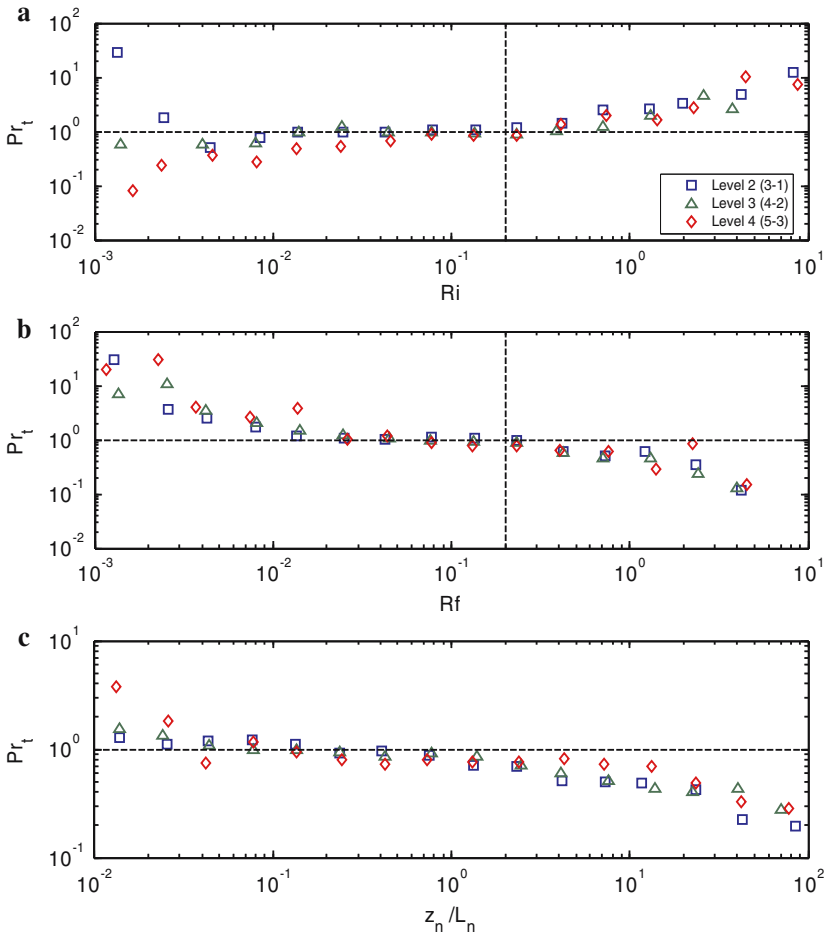

Fig. 2 Plots of the bin-averaged turbulent Prandtl number (bin medians) as functions of (**a**) Ri, (**b**) Rf, and (**c**) z_n/L_n (bin means) during the 11 months of the SHEBA measurements for level $n = 2$–4. Vertical gradients that appear in Pr_t, Ri, and Rf are based on the linear interpolation of mean wind speed and potential temperature derived from the two adjoining levels $n-1$ and $n+1$. For example, the gradients at level 2 are based on the temperature and wind speed differences between levels 3 and 1

relationship is sought have built-in correlation because of their shared variables (e.g., Hicks 1978; Mahrt et al. 1998; Andreas and Hicks 2002; Klipp and Mahrt 2004; Lange et al. 2004; Baas et al. 2006 and references therein). Self-correlation is also referred to as artificial, fictitious or spurious correlation. As an illustration, note that the turbulent Prandtl number is correlated to the gradient and flux Richardson numbers because $\mathrm{Pr}_t = \mathrm{Ri}/\mathrm{Rf}$ (see Eqs. 1, 3, and 5); that is, Pr_t varies proportionally with Ri but inversely with Rf (cf. Fig. 1a, b).

Usually, the self-correlation problem is discussed for plots of φ_m, φ_h, and variances vs. ζ primarily because of the shared friction velocity (e.g., Andreas and Hicks 2002; Baas et al. 2006). But self-correlation arises in several other atmospheric surface-layer applications (e.g., Andreas et al. 2006). In our particular application, self-correlation

occurs in plots of Pr_t vs. Ri (Figs. 1a, 2a) because of the shared vertical gradients of mean wind speed and potential temperature. Furthermore, random variability in both shared variables leads to increasing Pr_t with increasing Ri. According to Eqs. 1 and 3, increasing $\mathrm{d}\theta/\mathrm{d}z$ leads to increases in both Pr_t and Ri; and increasing $\mathrm{d}U/\mathrm{d}z$ leads to decreases in both Pr_t and Ri. Therefore, the self-correlation associated with variations in both $\mathrm{d}\theta/\mathrm{d}z$ and $\mathrm{d}U/\mathrm{d}z$ leads to the tendency for Pr_t to increase with increasing Ri, as demonstrated in Figs. 1a and 2a.

Similarly, in plots of Pr_t vs. ζ, random variability in the shared variables u_* and $\langle w'T'\rangle$ leads to decreasing Pr_t with increasing ζ, and vice versa (see Eqs. 1 and 3). Plots of Pr_t vs. Rf have three shared variables: $\langle u'w'\rangle$, $\langle w'T'\rangle$, and $\mathrm{d}U/\mathrm{d}z$ (see Eqs. 1 and 5). Random variability in two of them, $\langle u'w'\rangle$ and $\langle w'T'\rangle$, leads to decreasing Pr_t with increasing Rf, and vice versa; while variability in $\mathrm{d}U/\mathrm{d}z$ gives the opposite result: that is, increasing Pr_t with increasing Rf, and vice versa.

However, not all self-correlations are serious. The degree of self-correlation is related to the variation in the shared variables compared to those of the other (non-shared) variables, and it is described by the coefficient of variation $V_x = \sigma_x/\bar{X}$ (e.g., Klipp and Mahrt 2004), where the standard deviation, σ_x, and the mean value, $\bar{X}$, are the statistics for the whole dataset. According to the SHEBA data, a typical coefficient V_x (computed for median values) may be as much as $V_x \approx 1.2$ for $\langle u'w'\rangle$, $V_x \approx 0.8$ for $\langle w'T'\rangle$, $V_x \approx 0.3$ for $\mathrm{d}U/\mathrm{d}z$, and $V_x \approx 1.1$ for $\mathrm{d}\theta/\mathrm{d}z$. Thus, more serious self-correlation for SHEBA data is associated with variations in both $\langle u'w'\rangle$ and $\mathrm{d}\theta/\mathrm{d}z$.

Another sign of the self-correlation in Figs. 1 and 2 is associated with the behaviour of Pr_t for weakly stable conditions. According to Figs. 1 and 2, Pr_t decreases as $\mathrm{Ri} \to 0$ and $\mathrm{Pr}_t \approx 0.1$ at $\mathrm{Ri} \approx 0.001$ (Figs. 1a and 2a); while Pr_t increases as $\mathrm{Rf} \to 0$ and $\mathrm{Pr}_t \approx 10$ at $\mathrm{Rf} \approx 0.001$ (Figs. 1b and 2b). Yagüe et al. (2001, their Fig. 10a) found a similar discrepancy for small Ri in plots of $1/\mathrm{Pr}_t$ vs. Ri. Obviously, this experimental result contradicts the canonical limit that $\mathrm{Pr}_t \approx 1$ for neutral conditions. Thus, self-correlation severely influences functional dependencies between Pr_t and different stability parameters in Figs. 1 and 2.

To obtain a more reliable and independent picture of how the turbulent Prandtl number behaves over a wide range of stable conditions, we plot Pr_t vs. Ri_B, Eq. 6, in Fig. 3. Obviously, these plots have no built-in correlation. Vertical gradients that appear in Pr_t in Fig. 3 are based on fitting a second-order polynomial through the 1-h profiles similarly to Fig. 1. The bulk Richardson number in the upper panel (Fig. 3a) is based on the wind speed at reference level z_n ($n = 1 - 5$) and differences in the potential temperature and the specific humidity between the surface and the level z_n.

Whereas, the bulk Richardson number in the bottom panel (Fig. 3b) is based on the wind speed at median level z_m and differences between the surface and the level z_m, i.e., Pr_t at a level z_n ($n = 1-5$) is plotted vs. the bulk Richardson number with fixed z. Thus plotting Pr_t vs. $\mathrm{Ri}_{B\,m}$ in Fig. 3b provides information on the height dependence of the turbulent Prandtl number. According to the SHEBA data in Fig. 3, the Pr_t data are scattered around 1 for weakly stable conditions (around 0.01). The greater scatter of points in Fig. 3 for $\mathrm{Ri}_B < 0.01$ results from the relatively small sensible heat flux and unreliable temperature gradient measurements in near-neutral conditions.

With increasing stability, Pr_t decreases *on the average*, although Pr_t at different levels behaves variously. Figure 3b shows that in the range $0.01 < \mathrm{Ri}_{B\,m} < 0.03$, the turbulent Prandtl number decreases with increasing height for fixed $\mathrm{Ri}_{B\,m}$, i.e., $\mathrm{d}\,\mathrm{Pr}_t\,/\mathrm{d}z < 0$. Furthermore Pr_t at two lower levels is above 1: $\mathrm{Pr}_t(z_5) < \mathrm{Pr}_t(z_4) < \mathrm{Pr}_t(z_3) \approx 1 < \mathrm{Pr}_t(z_2) < \mathrm{Pr}_t(z_1)$. However, with further increasing stability, Pr_t at all levels tends to

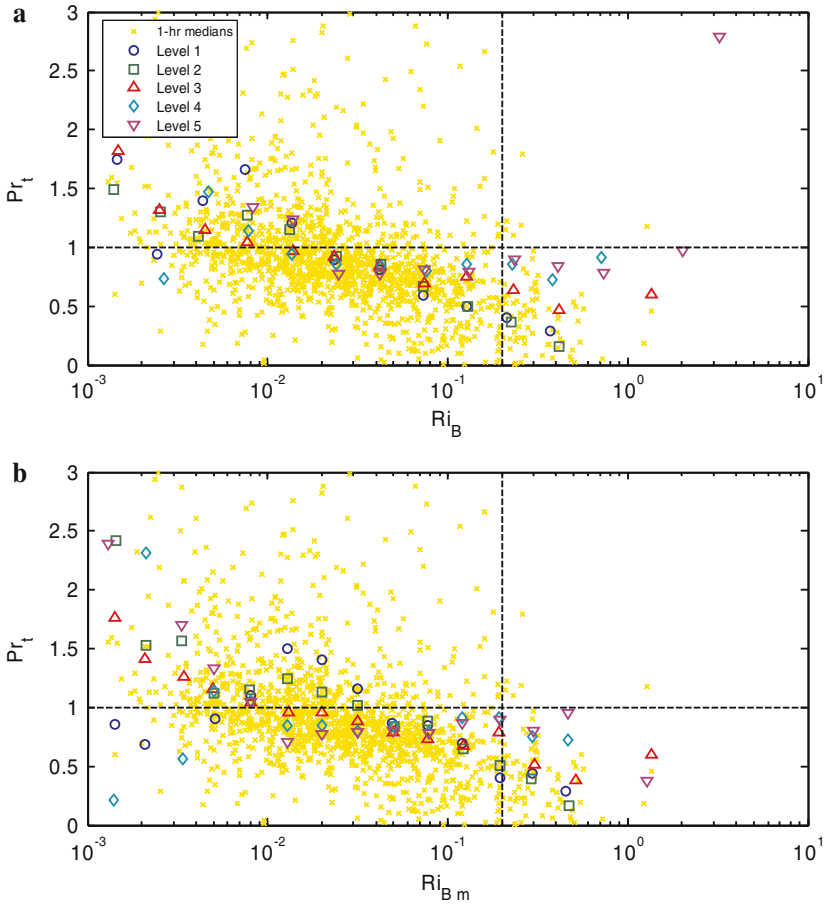

Fig. 3 Plots of the bin-averaged turbulent Prandtl (bin medians) number as functions of the bulk Richardson number (bin means) which is based on the (**a**) differences between the surface and reference level z_n (Ri_B) and (**b**) differences between the surface and median level z_m ($\mathrm{Ri}_{B\,m}$) during the 11 months of the SHEBA measurements. The vertical dashed lines correspond to the critical Richardson number, $\mathrm{Ri}_B = 0.2$. Individual 1-h averaged data based on the median fluxes for the five levels are shown as background crosses

be less than 1 in the subcritical regime, $\mathrm{Ri}_B < 0.2$ (see more discussion in the next Section). Thus Fig. 3 supports the conclusion that Pr_t on the average decreases with increasing stability for the SHEBA data. It seems that the trend in the Pr_t–Ri data in the SHEBA set (Figs. 1a and 2a) results strictly from self-correlation.

We suspect that self-correlation also influenced the conclusion, reported by others, that Pr_t increases with increasing Ri. Another notable example of self-correlation is the suggestion that the von Kármán constant depends on the roughness Reynolds number. Andreas et al. (2006) found recently that artificial correlation seems to explain the tendency for the von Kármán constant to decrease with increasing roughness Reynolds number in the atmospheric surface layer (i.e., Frenzen and Vogel 1995a, b; Oncley et al. 1996). According to Andreas et al. (2006) the von Kármán constant is, indeed, constant at 0.38–0.39.

In any event, analyzing self-correlation should be central for estimating how Pr_t behaves in the stable boundary layer because built-in correlation is unavoidable in the relations between Pr_t and the stability parameters Ri, Rf, and ζ. Ultimately, we must separate the effects of self-correlation and the physics on the dependency between Pr_t and the stability parameters.

4 Case Study

Although plots of averaged turbulent Prandtl number vs. different stability parameters are useful for qualitative analyses, additional detailed information can be obtained from time series of the turbulent Prandtl number and other relevant variables plotted for different conditions. Note that such plots by definition contain no built-in correlation. Typical time series of hourly averaged Pr_t, z_n/L_n, and Ri_B for moderately and very stable conditions during the dark period at SHEBA are shown in Figs. 4 and 5, respectively. Note that for data presented in Fig. 4, wind speed, wind direction, air temperature, and turbulent fluxes at each level (not shown) are approximately constant during 1997 YD (Year Day) 344.1–345.3 which lasts longer than 1 day. Therefore, z_n/L_n, and Ri_B (Fig. 4b, c) are also approximately constant for this period. At high latitudes, especially during the polar night, stable conditions are long lasting and can reach quasi-stationary states (e.g., Fig. 4) compared to measurements in the traditional nocturnal boundary layer in mid-latitudes. Such long-lived SBLs eventually can reach very stable states (e.g., Fig. 5).

Three-day's evolution of the turbulent Prandtl number, z_n/L_n, and the bulk Richardson for moderately stable conditions is shown in Fig. 4. It is particularly remarkable that the turbulent Prandtl number decreases with increasing height (Fig. 4a). In addition, Pr_t at levels 4 and 5 is systematically less than 1, whereas Pr_t at the two lower levels tends to be above 1 (Pr_t at level 3 is basically scattered around 1). Similar behaviour of Pr_t during SHEBA also has been observed at other times, for example, during 1998, YD 13–15, 52–53, 65–67, 181.5–182.5, 201–203.

Figure 4a supports the result $\mathrm{d}\,\mathrm{Pr}_t/\mathrm{d}z < 0$ for $0.01 < \mathrm{Ri}_{B\,m} < 0.03$ presented in Fig. 3b. This finding is also in good agreement with Howell and Sun (1999) measurements and LES simulations by Basu and Porté-Agel (2006). Howell and Sun (1999) found on average that Pr_t estimates at the 3-m level are higher than at the 10-m level. According to Basu and Porté-Agel's (2006) study, $\mathrm{Pr}_t \approx 0.7$ inside the boundary layer (up to 150 m), but values of Pr_t increase to ~ 1 in the surface layer (Ibid. p. 2082). The result $\mathrm{d}\,\mathrm{Pr}_t/\mathrm{d}z < 0$ indicates that, for the stability range $0.01 < \mathrm{Ri}_{B\,m} < 0.03$, turbulent momentum transfer is relatively more efficient near the surface. It should be mentioned that measurements at two lower levels may be influenced by a surface flux footprint effect or a blowing snow effect (see Fig. 6 and relevant discussion in Grachev et al. 2007).

Figure 5 shows a typical 1-day time series of Pr_t, z_n/L_n, and Ri_B for the very stable conditions observed during December 27–28, 1997 (YD 361–363). The data are based on 1-h averaging. Time series of the basic meteorological variables and turbulent fluxes for YD 361.8–363 (Fig. 5) can be found in Grachev et al. (2003, their Fig. 1). According to Fig. 5a, the turbulent Prandtl number for the very stable conditions tends mainly to be less than 1 at all levels. Similar time series of Pr_t for the very stable conditions observed during SHEBA also can be found on 1998 YD 56, 64–65, and

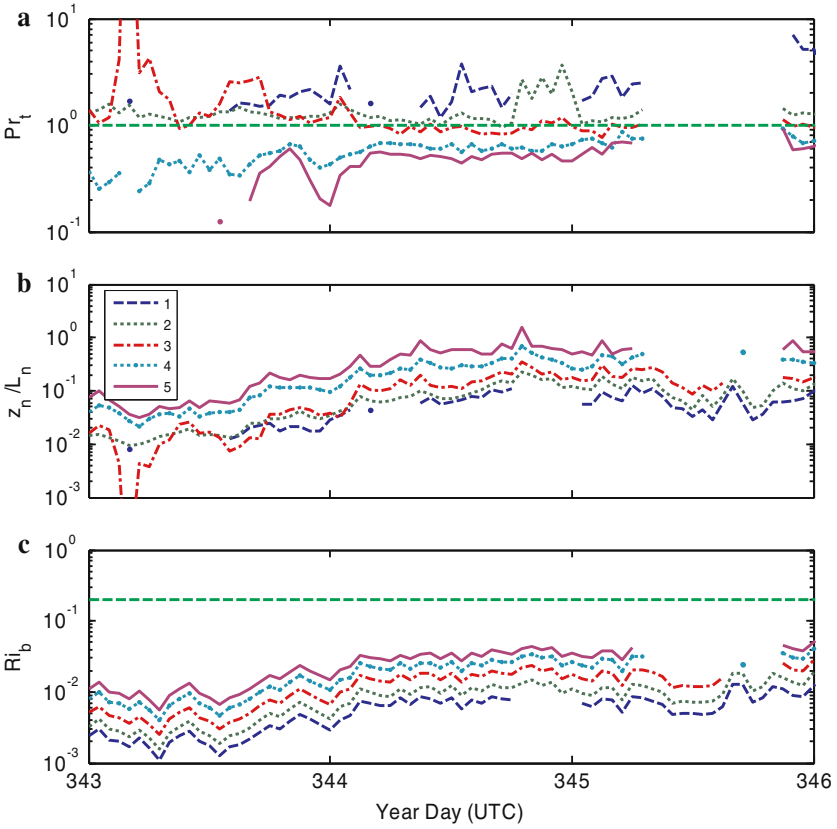

Fig. 4 Time series of the (**a**) the turbulent Prandtl number, (**b**) z_n/L_n, and (**c**) the bulk Richardson number measured at the five levels during moderately stable conditions, 1997 year days 343–346 (December 9–12, 1997 UTC). The data are based on 1-h averaging. The horizontal dashed line in the bottom panel correspond, to the critical Richardson number, $\mathrm{Ri}_B = 0.2$

142–143 among others [see also Fig. 2 in Grachev et al (2003) for YD 142–143 time series].

Although *on average* the turbulent Prandtl number decreases with increasing stability and $\mathrm{Pr}_t < 1$ in the very stable case (Fig. 3a), our study does not find that $\mathrm{Pr}_t < 1$ is a general result for the SBL. One may speculate that Pr_t generally does not have a universal behaviour in the stable atmospheric boundary layer in the framework of the Monin–Obukhov similarity. As mentioned above, Pr_t describes the difference in turbulent transfers of momentum and sensible heat. Similarity in the turbulent mixing of momentum and heat suggests that $\mathrm{Pr}_t \approx 1$. However, physical processes overlooked in Monin–Obukhov similarity theory (e.g., internal gravity waves, Kelvin–Helmholtz billows, an upside-down boundary layer, radiative flux divergence, etc.) may increase only the momentum flux ($\mathrm{Pr}_t > 1$), only the heat flux ($\mathrm{Pr}_t < 1$), or may produce a mixed effect and therefore violate similarity.

Eleven months of multi-level measurements during SHEBA cover a wide range of stability conditions and can shed light on the discrepancy of Pr_t measurements in the literature (see Sect. 1). In addition to the self-correlation problem discussed

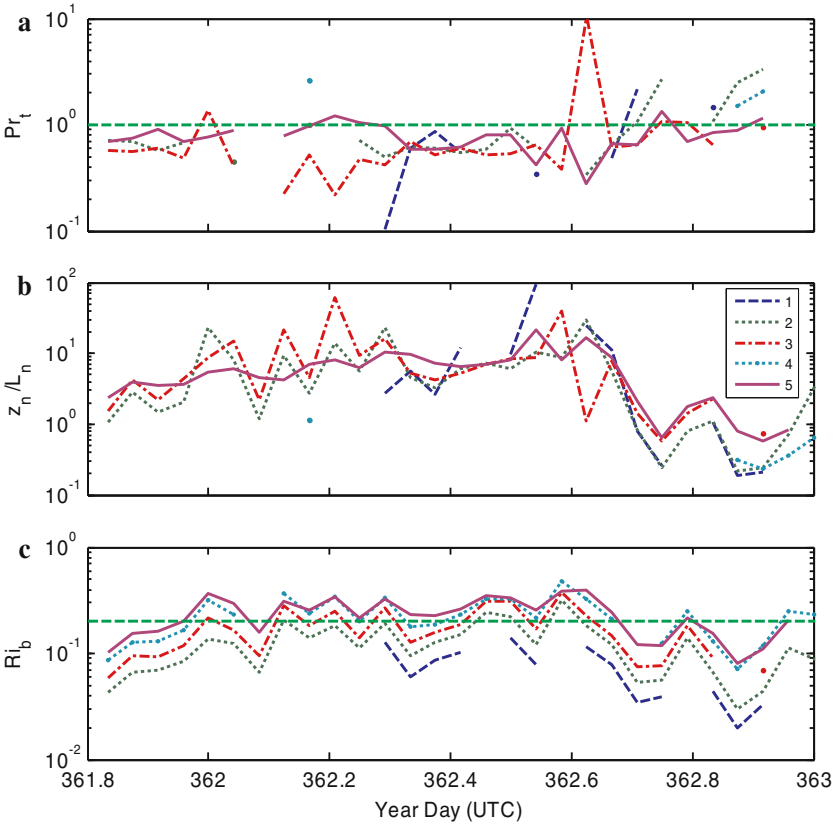

Fig. 5 Same as Fig. 4 but for data obtained during very stable conditions, 1997 year days 361–362 (December 27–28, 1997 UTC)

in Sect. 3, use of the limited datasets may be responsible for the discrepancy. For example, measurements only at heights less than 4 m (levels 1 and 2) for the limited stability range $\mathrm{Ri}_{B\,m} < 0.03$ result in $\mathrm{Pr}_t > 1$ (see Figs. 3b and 4). At the same time, Pr_t is systematically less than 1 for measurements at heights higher than 4 m (levels 3–5). As mentioned earlier, the *whole* SHEBA dataset *on the average* suggests that the turbulent Prandtl number decreases with increasing stability and $\mathrm{Pr}_t < 1$ in the very stable regime for all levels.

5 Conclusions

The turbulent Prandtl number in the SBL is discussed based on measurements made during SHEBA. Plots of Pr_t vs. Ri (as well as vs. Rf and ζ) for individual 1-h observations and relevant conventional bin-averaged values of the individual quantities suffer severely from self-correlation because of the shared variables. As a result, such analyses conceal any real physical correlation. For example, plots of Pr_t vs. different stability parameters for the same dataset give conflicting dependencies (Figs. 1 and 2). The turbulent Prandtl number increases with increasing stability if Pr_t is plotted

vs. Ri; but at the same time, Pr_t decreases with increasing stability if Pr_t is plotted vs. Rf or vs. $\zeta = z/L$. In addition, the data fail to agree with the canonical value $\mathrm{Pr}_t \approx 1$ for weakly stable conditions (Figs. 1a, b, 2a, b).

In contrast, plots of Pr_t vs. the bulk Richardson number, which have no built-in correlation, show that *on the average*, at least for the SHEBA data, Pr_t decreases with increasing stability and $\mathrm{Pr}_t < 1$ for all levels in the very stable cases (Fig. 3). However, the turbulent Prandtl number has more intricate behaviour for specific stability ranges and heights (Figs. 4 and 5). It is conceivable that the turbulent Prandtl number does not have a universal behaviour and $\mathrm{Pr}_t < 1$ is not a general result in the stable atmospheric boundary layer.

Acknowledgements The U.S. National Science Foundation supported this work with awards to the NOAA Environmental Technology Laboratory (now Earth System Research Laboratory) (OPP-97-01766), the Cooperative Institute for Research in Environmental Sciences (CIRES), University of Colorado (OPP-00-84322, OPP-00-84323), the U.S. Army Cold Regions Research and Engineering Laboratory (OPP-97-02025, OPP-00-84190), and the Naval Postgraduate School (OPP-97-01390, OPP-00-84279). The U.S. Department of the Army also supported ELA through Project 611102T2400. Thanks to all who participated in conversations which we held during the NATO Advanced Research Workshop (ARW) in Dubrovnik, Croatia, 18–22 April 2006, about the stability dependence of the turbulent Prandtl number in the atmospheric stable boundary layer. Special thanks go to Igor Esau for initiating that discussion.

References

Andreas EL (2002) Parameterizing scalar transfer over snow and ice: a review. J Hydormeterol 3:417–432

Andreas EL, Hicks BB (2002) Comments on 'Critical test of the validity of Monin-Obukhov similarity during convective conditions'. J Atmos Sci 59:2605–2607

Andreas EL, Claffey KJ, Jordan RE, Fairall CW, Guest PS, Persson POG, Grachev AA (2006) Evaluations of the von Kármán constant in the atmospheric surface layer. J Fluid Mech 559:117–149

Baas P, Steeneveld GJ, van de Wiel BJH, Holtslag AAM (2006) Exploring self-correlation in flux-gradient relationships for stably stratified conditions. J Atmos Sci 63(11):3045–3054

Basu S, Porté-Agel F (2006) Large-eddy simulation of stably stratified atmospheric boundary layer turbulence: a scale-dependent dynamic modeling approach. J Atmos Sci 63(8):2074–2091

Beare RJ, MacVean MK, Holtslag AAM, Cuxart J, Esau I, Golaz J-C, Jimenez MA, Khairoutdinov M, Kosovic B, Lewellen D, Lund TS, Lundquist JK, McCabe A, Moene AF, Noh Y, Raasch S, Sullivan P (2006) An intercomparison of large-eddy simulations of the stable boundary layer. Boundary-Layer Meteorol 118(2):247–272

Beljaars ACM, Holtslag AAM (1991) Flux parameterization over land surfaces for atmospheric models. J Appl Meteorol 30:327–341

Frenzen P, Vogel CA (1995a) On the magnitude and apparent range of variation of the von Kármán constant in the atmospheric surface layer. Boundary-Layer Meteorol 72:371–392

Frenzen P, Vogel CA (1995b) A further note 'On the magnitude and apparent range of variation of the von Kármán constant'. Boundary-Layer Meteorol 73:315–317

Grachev AA, Fairall CW, Persson, POG, Andreas EL, Guest PS, Jordan RE (2003) Turbulence decay in the stable arctic boundary layer. In: seventh conference on polar meteorology and oceanography and joint symposium on high-latitude climate variations. Amer. Meteorol. Soc., Hyannis, Massachusetts, Preprint CD-ROM

Grachev AA, Fairall CW, Persson POG, Andreas EL, Guest PS (2005) Stable boundary-layer scaling regimes: the SHEBA data. Boundary-Layer Meteorol 116(2):201–235

Grachev AA, Andreas EL, Fairall CW, Guest PS, Persson POG (2007) SHEBA flux-profile relationships in the stable atmospheric boundary layer. Boundary-Layer Meteorol (in press) DOI: 10.1007/s10546-007-9177-6

Hicks BB (1978) Comments on 'The characteristics of turbulent velocity components in the surface layer under convective conditions by H A Panofsky, et al. Boundary-Layer Meteorol 15(2):255–258

Howell JF, Sun J (1999) Surface-layer fluxes in stable conditions. Boundary-Layer Meteorol 90(3):495–520
Kim J, Mahrt L (1992) Simple formulation of turbulent mixing in the stable free atmosphere and nocturnal boundary layer. Tellus 44(5):381–394
Klipp CL, Mahrt L (2004) Flux-gradient relationship, self-correlation and intermittency in the stable boundary layer. Quart J Roy Meteorol Soc 130(601):2087–2103
Kondo J, Kanechika O, Yasuda N (1978) Heat and momentum transfers under strong stability in the atmospheric surface layer. J Atmos Sci 35:1012–1021
Lange B, Johnson HK, Larsen S, Højstrup J, Kofoed-Hansen H, Yelland MJ (2004) On detection of a wave age dependency for the sea surface roughness. J Phys Oceanogr 34(6):1441–1458
Mahrt L, Sun J, Blumen W, Delany T, Oncley S (1998) Nocturnal boundary-layer regimes. Boundary-Layer Meteorol 88:255–278
Monin AS, Yaglom AM (1971) Statistical fluid mechanics: mechanics of turbulence, vol. 1. MIT Press, Cambridge, MA pp 769
Monti P, Fernando HJS, Princevac M, Chen WC, Kowalewski TA, Pardyjak ER (2002) Observation of flow and turbulence in the nocturnal boundary layer over a slope. J Atmos Sci 59(17):2513–2534
Ohya Y (2001) Wind tunnel study of atmospheric stable boundary layers over a rough surface. Boundary-Layer Meteorol 98(1):57–82
Oncley SP, Friehe CA, Larue JC, Businger JA, Itswiere EC, Chang SS (1996) Surface-layer fluxes, profiles, and turbulence measurements over uniform terrain under near-neutral conditions. J Atmos Sci 53:1029–1044
Persson POG, Fairall CW, Andreas EL, Guest PS, Perovich DK (2002) Measurements near the atmospheric surface flux group tower at SHEBA: near-surface conditions and surface energy budget. J Geophys Res 107(C10):8045. DOI: 10.1029/2000JC000705
Strang EJ, Fernando HJS (2001) Vertical mixing and transports through a stratified shear layer. J Phys Oceanog 31(8):2026–2048
Sukoriansky S, Galperin B, Perov V (2006) A quasi-normal scale elimination model of turbulence and its application to stably stratified flows. Nonlinear Processes Geophys 13(1):9–22
Ueda H, Mitsumoto S, Komori S (1981) Buoyancy effects on the turbulent transport processes in the lower atmosphere. Quart J Roy Meteorol Soc 107(453):561–578
Yagüe C, Maqueda G, Rees JM (2001) Characteristics of turbulence in the lower atmosphere at Halley IV Station, Antarctica. Dyn Atmos Ocean 34:205–223
Zilitinkevich SS (2002) Third-order transport due to internal waves and non-local turbulence in the stably stratified surface layer. Quart J Roy Meteorol Soc 128:913–925
Zilitinkevich S, Calanca P (2000) An extended similarity-theory for the stably stratified atmospheric surface layer. Quart J Roy Meteorol Soc 126:1913–1923